Optoelectrofluidic enhanced immunoreaction based on optically-induced dynamic AC electroosmosis

Dongsik Han and Je-Kyun Park*

We report a novel optoelectrofluidic immunoreaction system based on electroosmotic flow for enhancing antibody–analyte binding efficiency on a surface-based sensing system. Two conventional indium tin oxide glass slides are assembled to provide a reaction chamber for a tiny volume of sample droplet (~5 μL), in which the top layer is employed as an antibody-immobilized substrate and the bottom layer acts as a photoconductive layer of an optoelectrofluidic device. Under the application of an AC voltage, an illuminated light pattern on the photoconductive layer causes strong counter-rotating vortices to transport analytes from the bulk solution to the vicinity of the assay spot on the glass substrate. This configuration overcomes the slow immunoreaction problem of a diffusion-based sensing system, resulting in the enhancement of binding efficiency via an optoelectrofluidic method. Furthermore, we investigate the effect of optically-induced dynamic AC electroosmotic flow on optoelectrofluidic enhancement for surface-based immunoreaction with a mathematical simulation study and real experiments using immunoglobulin G (IgG) and anti-IgG. As a result, dynamic light patterns provided better immunoreaction efficiency than static light patterns due to effective mass transport of the target analyte, resulting in an achievement of 2.18-fold enhancement under a growing circular light pattern compared to the passive mode.

Introduction

Surface-based molecular sensing systems, measuring the concentration of target analytes in sample solution at the reaction surface with receptors, have been widely utilized as a powerful analytical tool for identification of target molecules with various applications. Microarray technologies, which sense target molecules such as nucleic acids and proteins, have been mostly employed in genomics and proteomics research.[1,2] Meanwhile, several immunoassay methods, based on specific binding between the antibody and analyte, have been actively developed for detecting disease biomarkers.[3,4] In these diagnostic fields, highly sensitive detection of target analytes is a significant issue particularly in handling small-volume samples. A critical factor to achieve excellent detecting performance in surface-based sensing systems is the transport of target molecules in sample solution to a reaction surface where receptors are immobilized.[5] However, conventional surface-based detecting systems require a long incubation time from hours to days to get meaningful assay results because the surface reaction of receptors and target molecules depends on random molecular diffusion, resulting

in low assay performance due to diffusion limitations. Therefore, the ability for real-time highly sensitive detection of target molecules has been required to realize a practical tool for rapid sensing.

In this regard, mass transport phenomena of surface-based systems have been actively studied by numerical simulation.[6,7] Besides, several microfluidic technologies such as acoustic mixers[8] and hydrodynamic mixers[9] have been widely applied to improve mixing efficiency in sample solution for enhancement of binding efficiency between receptors and target molecules by overcoming diffusion limitations. Over the past decade, microfluidic systems based on AC electrokinetics have also been proposed to develop a mixing method for molecular detection. In particular, DNA hybridization and protein immunoassays were enhanced by electrically-driven convective flow.[10,11] These microfluidic technologies can minimize costly reagent consumption. In addition, these systems utilize electrically-induced vortexes under non-uniform electric fields to provide rapid mass transport of molecules which overcomes diffusion limitations. However, elaborate fabrication of micro-dimensional electrode arrangements for generating a non-uniform electric field is not simple and requires a time-consuming and costly process. Moreover, fixed electrode construction provides only a limited flow pattern, which restricts practical applications with various types of assay format in biological and chemical fields.

Department of Bio and Brain Engineering, Korea Advanced Institute of Science and Technology (KAIST), 291 Daehak-ro, Yuseong-gu, Daejeon 34141, Republic of Korea. E-mail: jekyun@kaist.ac.kr; Fax: +82 42 350 4310; Tel: +82 42 350 4315

Recently, optoelectrofluidics based on electrokinetic phenomena under a non-uniform AC electric field induced by an optical regime has been actively investigated.[12–14] Particularly, in biological and chemical fields, optically-induced electrokinetics has been considered as a fascinating technology because the dominant principle among AC electrokinetics, including dielectrophoresis, AC electroosmosis (ACEO), can be selectively generated at the required position in a user-friendly optical manner, resulting in the generation of programmable and on-demand manipulation. Thanks to these advantages, different-sized particles were selectively concentrated, separated and patterned.[14] Besides, the optoelectrofluidic manipulations of biological or chemical objects such as protozoan cells,[15] oocytes,[16] blood cells,[17] macromolecules[18] and two-phase droplets[19] were demonstrated. In addition, an in situ surface-enhanced Raman scattering signal measurement system[20] and a bead-based immunoassay system have been reported.[21]

In this study, we investigate the effect of optically-induced ACEO flow that provides programmed and on-demand strong local vortexes on the binding efficiency with mass transport of target molecules toward a reaction surface by a simulation study and real experiments using a model reaction set of immunoglobulin G (IgG) and anti-IgG. Compared to the previously reported optoelectrofluidic immunoassay system, the proposed system focuses on the effect of various types of optically-induced ACEO flows on reaction performance to overcome the diffusion limitation problem of conventional surface-based reaction systems rather than bead-based immunoassays.[21] In addition, the proposed optoelectrofluidic enhancing method is compared to the passive mode where molecules are transported in only a random diffusion manner with respect to mass transport and enhancement of the surface reaction rate. Furthermore, optically-induced ACEO flows with several types of light patterns such as different-sized light patterns, ring-type light patterns and temporally-changed dynamic light patterns are explored to understand enhancement of binding efficiency with mass transport phenomena for surface-based sensing platforms.

Materials and methods

Chemicals and reagents

Quantum dot (with fluorescence emission at 605 nm) conjugated IgGs were purchased from Thermo Fisher Scientific. Anti-IgG, bovine serum albumin (BSA), Tween 20, glutaraldehyde solution, (3-aminopropyl)trimethoxysilane (APTMS), and ethanol were obtained from Sigma-Aldrich. Phosphate-buffered saline (PBS) containing 0.05% (w/v) Tween-20 (PBST) was used as a washing buffer. A buffer solution containing 1% BSA was used as a blocking solution. Diluted PBS (25 μS cm^{-1}) was used as a reaction buffer. Doubly deionized water was used throughout the experiments.

Device fabrication

To fabricate an optoelectrofluidic device, glass substrates coated with indium tin oxide (ITO) were used as two transparent electrodes. The top transparent electrode was used for assay spot preparation and the bottom electrode was a photoconductive layer-deposited ITO-glass substrate. Here, the photoconductive layer was fabricated by sequentially depositing three layers on ITO-glass by a plasma enhanced chemical vapor deposition method in a single chamber reactor: (1) a 50 nm thick heavily doped hydrogenated amorphous silicon (n$^+$ a-Si:H) layer; (2) a 1 μm-thick intrinsic hydrogenated amorphous silicon (intrinsic a-Si:H) layer; (3) a 20 nm-thick silicon nitride (SiN$_\chi$) layer. For the electrical connection, a part was etched by a reactive ion etching method to reveal the ITO layer. Detailed fabrication processes have been described in the previous paper.[17]

Preparation of assay spots on the glass substrate

Preparation of assay spots was carried out by immobilizing capture antibodies on an ITO-glass slide. The ITO-glass slide was cleaned by sonicating in acetone solution for 10 min and isopropyl alcohol solution for 10 min serially, and was rinsed successively with deionized water three times. After the glass slide was dried at room temperature, the cleaned slide was immersed in ethanol with 10% APTMS at room temperature for 1 h to form self-assembled monolayers (SAMs) of aminosilane, and rinsed with ethanol, the reaction buffer and deionized water three times. It was then dried at room temperature and heat-treated at 120 C$^\circ$ for 5 h. After cooling, amino groups formed on the ITO-glass slide were activated with 2.5% glutaraldehyde solution for 1 h at room temperature, dipped into deionized water for 1 min, and dried at room temperature. Assay spots, which consist of capture antibodies, were spotted onto the activated-glass slide using a pin-type microarrayer (OmniGrid Accent™ Microarrayer; Digilab Inc., MA, USA) with 200 μL of antibody solution (0.2 mg mL^{-1} for anti-IgG).

System configuration

The experimental system is illustrated in Fig. 1. 5 μL of sample droplet was placed in a 30 μm-height liquid chamber between the transparent glass slide with assay spots (with a diameter of 200 μm) and the photoconductive layer-deposited glass slide, which covered a circular region with a diameter of 1.5 cm. An AC voltage generated from a function generator (AFG310; Tektronix, OR, USA) was applied across the ITO electrodes. A light source (2.2 $\times$ 10^4 lx) was patterned through a liquid crystal display, which could be easily controlled by a common software program installed on a laptop. The results of immunoreaction within the optoelectrofluidic device could be observed using a fluorescence microscope (IX72; Olympus, Japan) and captured by a charge-coupled device (DP72; Olympus, Tokyo, Japan).
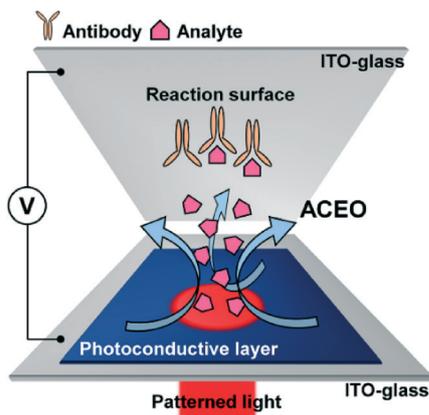
Fig. 1 Schematic illustration of optoelectrofluidic immunoreaction system. An optoelectrofluidic device containing a sample droplet is controlled by a patterned light. When a light pattern is projected onto the assay spot under an AC voltage, a non-uniform electric field is formed in the 30 μm-height chamber. This non-uniform electric field generates AC electroosmosis (ACEO) which transports analytes with strong convective flow into the reaction surface to enhance immunoreaction.

Optoelectrofluidic immunoreaction procedure

First, excess active sites of the antibody-immobilized glass slide were blocked with 1% BSA solution for 30 min to limit nonspecific binding, and the glass slide was rinsed with the washing buffer. After assembling the antibody-immobilized glass slide with the photoconductive layer-coated glass slide to form an optoelectrofluidic device, an antibody–antigen reaction was performed in an optoelectrofluidic enhancing manner where a light pattern was projected on the assay spot with an applied AC voltage with 15 V_{pp} at 10 kHz between two glass slides for 10 min. Following the reaction, the reacted glass slide was detached from the optoelectrofluidic device and then was serially rinsed with PBST, PBS and deionized water for removing unbound analytes. After the final washing step, the reacted glass slide was dried, and the results were imaged for data acquisition by a fluorescence microscope.

Results and discussion

Optically-induced ACEO

AC electroosmosis is one of the electrohydrodynamic phenomena under an AC electric field, which is caused by the motion of ions along the surface of the electrode in an electric double layer by a tangential electric field. In order to study optoelectrofluidic phenomena induced in the proposed system, a commercial software program, CFD-ACE+ (ESI Group, Huntsville, AL, USA), was used for computational fluidic dynamic (CFD) analysis. In an optoelectrofluidic device, when a light pattern with a diameter of 200 μm is projected onto the photoconductive layer deposited on an ITO-glass slide (Fig. 2(a)), the irradiated region that acts as a virtual electrode becomes conductive, resulting in a non-uniform electric field between ITO-glass slides under an AC voltage
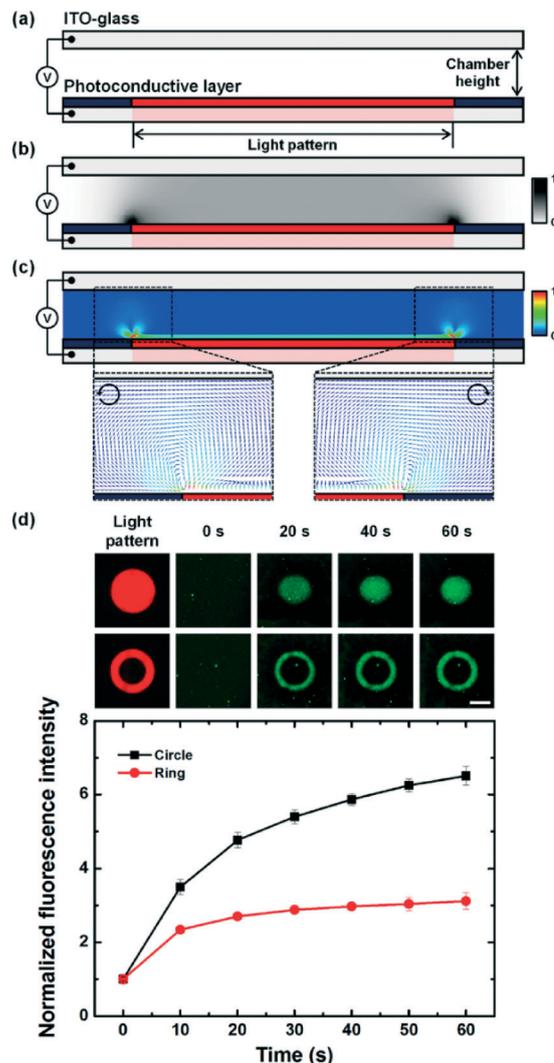

Fig. 2 Mathematical simulation and experimental results of the optically-induced AC electroosmotic (ACEO) flow. (a) Simulation design of the optoelectrofluidic device. A circular light pattern (200 μm in diameter) was irradiated on the photoconductive layer under an applied AC voltage of 15 Vpp at 10 kHz. (b) Numerical simulation of the electric field distribution. (c) Simulation of the electrically-driven fluid velocity. (d) Experimental results for the confirmation of optically-induced ACEO flow using nanoparticles. Error bars represent the standard deviation from duplicate experiments (scale bar: 100 μm, n = 3).

source (Fig. 2(b)). Under the non-uniform electric field, a pair of strong convective flows was generated (Fig. 2(c)), which is defined by

$$\langle v_{slip} \rangle_t = \frac{1}{2} \frac{\lambda_D}{\eta} \mathrm{Re}\left[\sigma_q E_t^* \right]$$

where λ_D is the Debye length, η is the fluid viscosity, σ_q is the charge contained in the Debye layer, and E_t is the tangential electric field.[22] Then, the electrically-driven body force creates the fluid's motion called ACEO. At the edges of the light pattern, the optically-induced ACEO flow shows a maximum velocity magnitude value of 2.7 mm s^{-1} with a pair of counter-rotating vortices (left: counter-clockwise, right:

clockwise) and a relatively lower velocity at the center of the light pattern. This induced-flow phenomenon can transport molecules to the center of the light pattern, which increases the local concentration of molecules *via* the strong flow with high velocity at the center of the light pattern. To investigate the formation of optically-induced ACEO in this system, experiments using fluorescent nanoparticles were performed (Fig. 2(d)). The existence of ACEO could be confirmed by observing the concentration of nanoparticles at the center of the optically-induced virtual electrode due to the pair of counter-rotating convective flows. Experimental results showed temporal changes in the concentration of nanoparticles at the irradiated region, indicating that an ACEO flow was successfully generated in an optical manner with the application of 15 V_{pp} at 10 kHz frequency. Besides, we also confirmed that the ACEO flow could be selectively generated at the irradiated region by applying a ring-type light pattern.

Optoelectrofluidic enhancing effect *via* optically induced ACEO

When the specific capture of target analytes based on immunoreaction is carried out by immobilized antibodies at the reaction surface, the reaction kinetics at the antibody-immobilized surface can be described as a two-step process: mass transport process and chemical reaction process.[7,23–25] Generally, immunoassays on surface-based biosensors rely on a diffusion-limited reaction, which means that transporting molecules to the reaction surface takes a longer time than immunoreaction on the reaction region. This mass-transport limitation due to the diffusion boundary layer has been considered as a critical problem to be overcome for practical applications of immunoassay technologies.

To solve this problem, we applied an optoelectrofluidic technology to enhance immunoreaction and carried out experiments to investigate the effect of optically induced electrokinetic flow (Fig. 3(a)). First, we explored the optoelectrofluidic enhancing effect on the aspect of mass transport by a mathematical simulation study (Fig. 3(b)). Under the passive mode where chemical reactions of the antibody and analyte were performed without the application of voltage and light pattern, molecules in the chamber were transported *via* only a random diffusion method. Therefore, the diffusion limitation problem of the surface-based immunoassay became intensified from the reaction surface as time passed, resulting in a low reaction rate. Meanwhile, the active mode where optically-induced electrokinetic vortices were generated at the reaction surface was applied to the assay spot; these counter-rotating strong vortices could actively transport molecules to the reaction region. Because target analytes could be continuously provided to the reaction surface with convective fluidic phenomena, the critical problem for a long reaction time due to the diffusion boundary layer of the passive
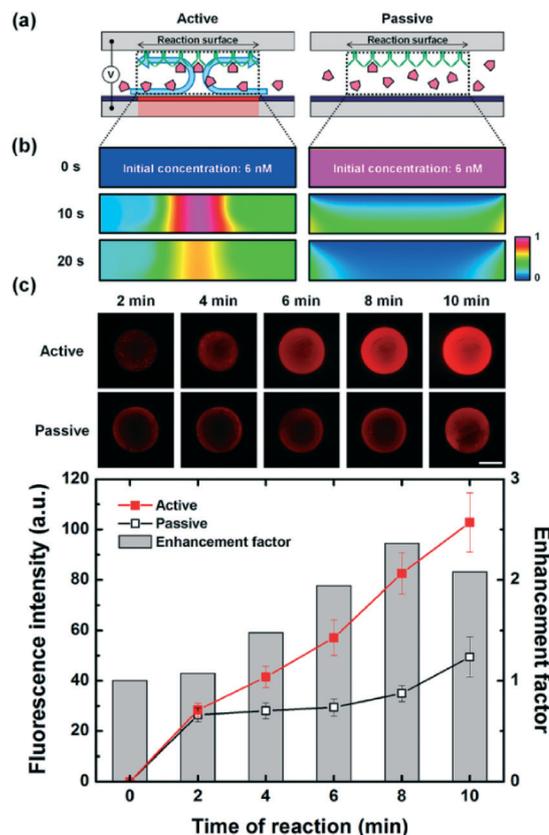

Fig. 3 Comparison of operation modes in an optoelectrofluidic device. (a) Schematic illustrations of optoelectrofluidic active and passive modes. (b) Simulation results of the temporal distribution change of analyte concentration under active and passive modes. (c) Fluorescence immunoreaction results and enhancement with respect to the optoelectrofluidic method. After constructing assay spots and blocking the surface with 1 mg mL^{-1} bovine serum albumin for 30 min, 20 nM IgG conjugated with quantum dot solution was loaded and a voltage of 15 V_{pp} was applied with the circular light pattern. The enhancement factor indicates the ratio of fluorescence intensity compared to the passive mode. Error bars represent the standard deviation from duplicate experiments (scale bar: 100 μm, n = 5).

mode was solved under the active mode. To investigate the optoelectrofluidic enhancing effect, heterogeneous immunoassays were performed (Fig. 3(c)). Experimental results showed similar binding rates for initial 2 min since the local concentrations of free analytes were enough to perform immunoreaction under both passive and active modes. However, as free analytes near the reaction surface were bound with receptors, an analyte depletion problem occurred in the passive mode due to the lack of mass transport, resulting in a slow reaction under the passive mode. On the other hand, the optoelectrofluidic method provided a rapid binding performance with more than two-fold enhancement factor with a 2.52-fold faster reaction velocity compared to the passive mode for 10 min, which indicated that the optically-induced ACEO flow could be an effective solution to overcome diffusion limitations of surface-based sensing systems.

Effect of size and shape of light patterns

Antibodies are generally spotted in the shape of a circle on a chemical-treated glass slide for a conventional surface-based immunoassay using a microarray-based technology. To investigate what type of light pattern effectively works on the circular-shaped assay spot, we carried out experiments for optoelectrofluidic immunoassays under applying different sized light patterns and ring-type light patterns using antibodies and a quantum dot-conjugated analyte. For enhancing immunoreaction, different sized circular light patterns were applied to generate optically-induced ACEO flow (Fig. 4(a)). According to mathematical simulation results, a 100% circular light pattern provided better mass transport efficiency than 50% and 150% light patterns (Fig. 4(b)). As a result, a 100% light pattern could enhance immunoreaction much better than others (Fig. 4(c)). Although an optoelectrofluidic enhancing effect occurred under all experimental conditions with different sizes of light patterns, the light pattern which has the same diameter as the assay spot could provide an optimized flow phenomenon to effectively cover the reaction region considering the characteristics of ACEO flow to concentrate molecules at the optically-irradiated region to reduce the analyte depletion problem.

Moreover, we applied ring-type light patterns with different thicknesses to investigate the effect of different formations of optically-induced vortices on reaction efficiency at the reaction surface compared with the circular-shaped light pattern (Fig. 4(d)). When a light pattern was irradiated on an optoelectrofluidic system, the vortex flow was generated at the interface between the light pattern and the non-irradiated region. We could generate two counter-rotating vortices under the circular-shaped light pattern (100%) due to the two interfaces in the direction of the diameter. Molecules were continuously transported to the light pattern under optically-induced ACEO flow followed by a supplement of local concentration of target molecules on the irradiated region. In contrast, the ring-shaped light patterns had four interfaces in the direction of the diameter, resulting in two couples of counter-rotating vortices at the edges of the light pattern. Each couple of vortices transported molecules to the irradiated region which is only a portion of the assay spot. For enhancing assay performance by overcoming the analyte depletion problem of the surface-based immunoassay, mass transport should be seriously considered. To investigate the mass transport of the analyte, a mathematical simulation study was conducted under a ring-type light pattern and a circular light pattern (Fig. 4(e)). According to our simulation results, mass transport of the target analyte could be effectively operated on the whole surface of the assay spot under the circular light pattern. On the other hand, the analyte depletion region at the reaction surface was shown to be relatively larger under the ring-type light pattern due to the interference between two pairs of counter-rotating vortices, which exerted a negative influence on the binding efficiency at the reaction surface. This difference of mass transport performance between light pattern types caused the variation of reaction efficiency, and the achievement of the most excellent
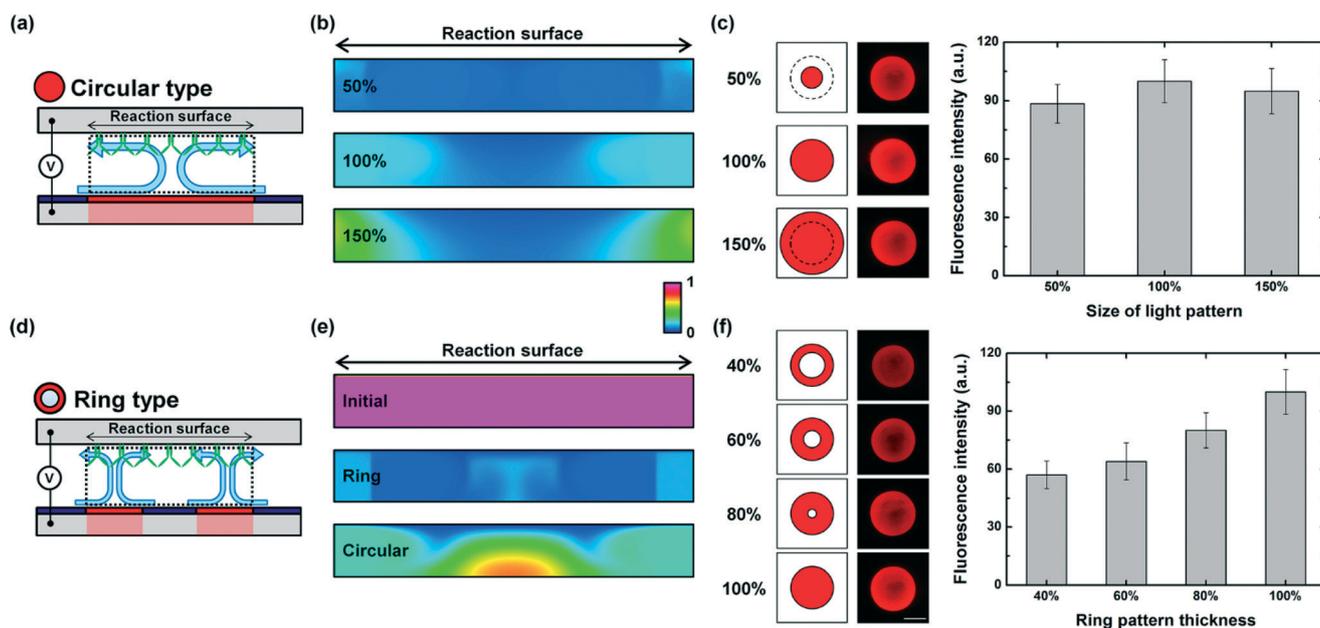

Fig. 4 Optoelectrofluidic enhanced immunoreaction results with respect to the size of the circular light pattern and the thickness of the ring pattern. (a) Schematic illustrations of optically–induced AC electroosmotic (ACEO) flow, (b) simulation results of analyte distribution, and (c) schematic illustration of projected light patterns and fluorescence immunoreaction results under a circular light pattern. (d) Schematic illustrations of optically–induced ACEO flow, (e) simulation results of analyte distribution, and (f) schematic illustration of projected light patterns and fluorescence immunoreaction results under a ring-type light pattern. Error bars represent the standard deviation from duplicate experiments (scale bar: 100 μm, n = 5).

enhancing effect was observed under the circular pattern (Fig. 4(f)).

Effect of dynamic light patterns

Blinking light patterns with different blinking periods were also applied to enhance surface immunoreaction to investigate the effect of optically-induced pulsed flow on the optoelectrofluidic enhancing effect. First, three types of blinking light patterns were utilized to generate optically induced ACEO flow (Fig. 5(a)). All blinking conditions have a homogeneous total time for 'On', but different unit times of blinking periods for 'On' and 'Off', including 1, 3, and 5 s, were applied for 10 min of incubation time to study the effect of unit times of blinking periods on reaction efficiency. Blinking light patterns could enhance immunoreaction on the reaction surface, resulting in about two-fold improvement for the binding efficiency of experimental results compared to the passive mode, which agreed with the enhancement factors from mathematical simulation results (Fig. 5(b)). Although a slightly better efficiency was shown from simulation studies under the blinking condition with a period of 3 s among the applied different blinking conditions, experimental results showed similar levels of reaction efficiency under all conditions, which implied that the unit time of blinking periods with a homogeneous total time for 'On' was not a significant factor in determining the reaction efficiency.

Moreover, blinking light patterns with different total times for 'On' such as 1/5 and 3/5 periods were employed to enhance immunoreaction for 10 min to investigate the effect of total time for 'On' on the reaction efficiency (Fig. 5(c)). According to the simulated results, immunoreactions were more improved as the total time for generating optically-induced ACEO flow increased, which could be also observed in experimental results (Fig. 5(d)). This tendency was thought to be caused by the difference in replenishment of free analytes to the reaction surface. While free analytes could be provided to the reaction surface from the surroundings via a pair of convective flows without any intermission under the static light pattern environment, the analyte depletion region might repetitively occur at the reaction surface during each 'Off' under blinking light patterns. In other words, continuous application of optically-induced ACEO provided better binding efficiency than an optoelectrofluidic method with a pulse. Therefore, although surface immunoreactions were enhanced under all active modes including blinking and static light patterns due to the rapid mass transport compared to the passive mode, the binding efficiency showed a tendency to improve as the total time for the active mode increased under a circular light pattern. From these results, the total time for the active mode, 'On', was considered as a significant factor to decide an enhancement of binding efficiency rather than the unit time of blinking periods.

We also applied temporal shrinking and growing light patterns with ring and circular shapes. First, dynamic ring-type light patterns were applied to investigate the effect of
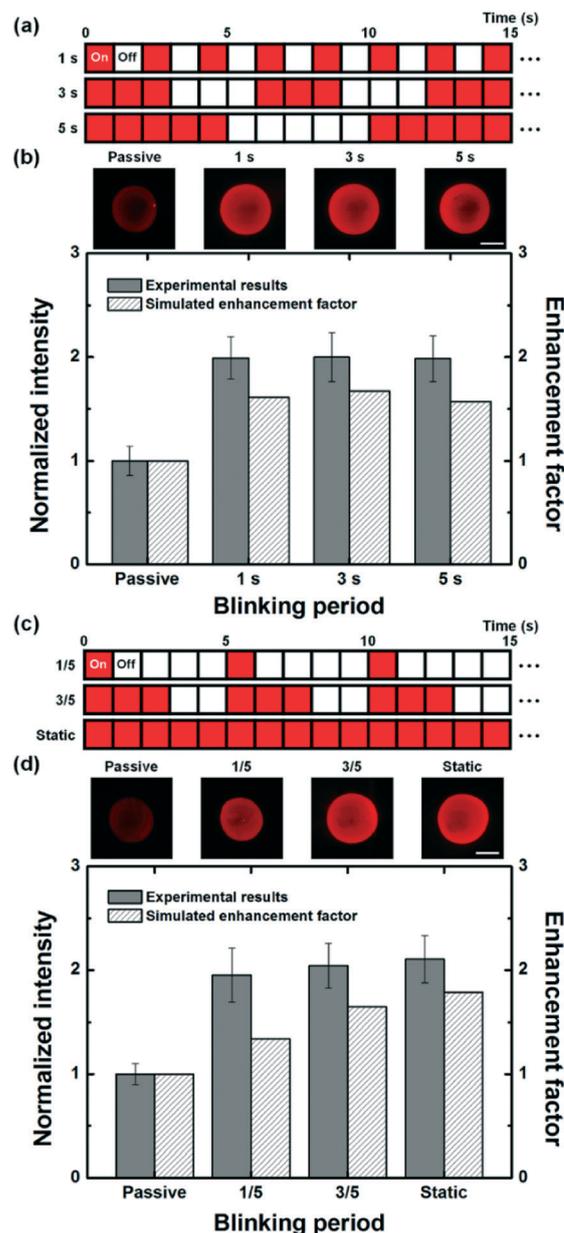

Fig. 5 Optoelectrofluidic enhanced immunoreaction results with respect to the types of blinking light pattern. (a, c) Schematic illustration of blinking period conditions for the light pattern. (b, d) Fluorescence immunoreaction results and simulated enhancement factors with respect to the blinking conditions. The simulated enhancement factor indicates the ratio of initial slope of temporal immunoreaction results compared to the passive mode. Error bars represent the standard deviation from duplicate experiments (scale bar: 100 μm, n = 5).

temporal changes of the location of two pairs of optically-induced convective flows on the reaction efficiency (Fig. 6(a)). As mentioned before, two pairs of convective flows under the static ring-type light pattern formed the analyte depletion region due to the interference, which acted on the surface immunoreaction as a distinct disadvantage, resulting in a relatively low binding efficiency (Fig. 4(f)). On the other hand, dynamic ring-type light patterns could remove the permanent
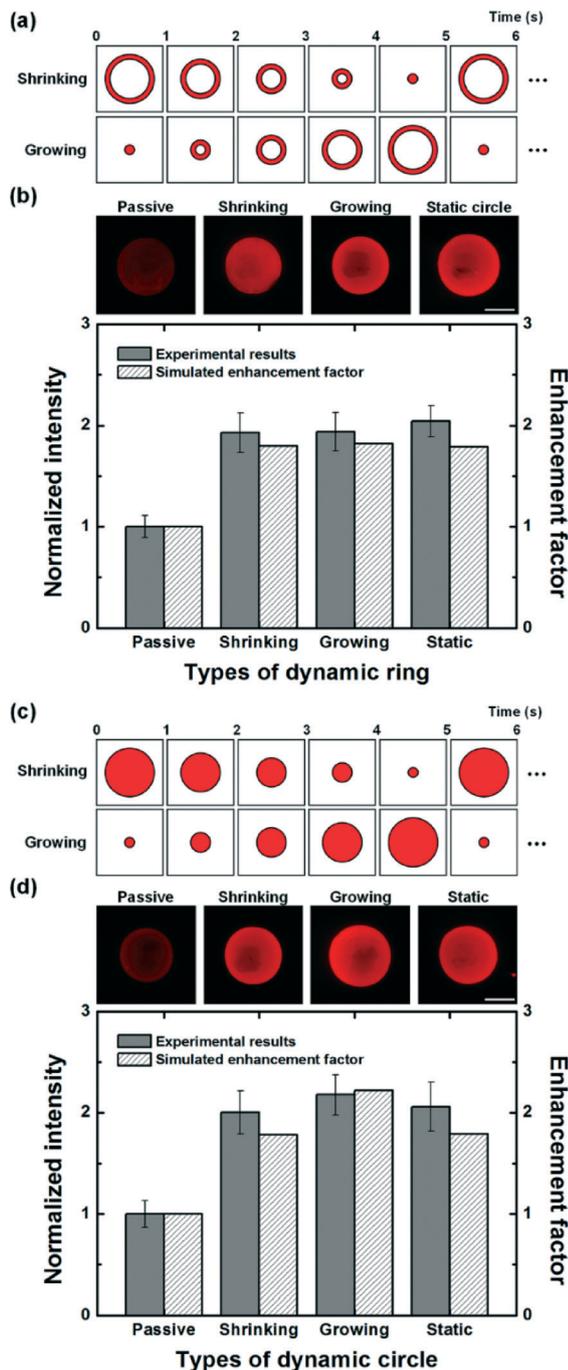
Fig. 6 Optoelectrofluidic enhanced immunoreaction results with respect to the types of dynamic light patterns including ring and circular types. (a, c) Schematic illustration of dynamic conditions for the light pattern. (b, d) Fluorescence immunoreaction results and simulated enhancement factors with respect to the dynamic light pattern condition. The simulated enhancement factor indicates the ratio of initial slope of temporal immunoreaction results compared to the passive mode. Error bars represent the standard deviation from duplicate experiments (scale bar: 100 μm, n = 5).

analyte depletion region of the static ring-type light pattern because the location of two pairs of vortices was continuously changed. Therefore, the problem occurring under the static

ring-type light pattern could be overcome, resulting in an improvement of binding efficiency under dynamic patterns (Fig. 6(b)). However, the enhancements were shown to be slightly smaller than 2, which could not exceed the efficiency under the static circular light pattern. Finally, dynamic circular light patterns were employed for enhancing immunoreaction to investigate the effect of dynamic shrinkage and growth of the circular light pattern (Fig. 6(c)). According to the experimental results, optoelectrofluidic enhancements were observed under all dynamic and static circular light patterns compared to the passive mode, but a difference in the enhanced binding efficiency was found (Fig. 6(d)). Based on mathematical simulation studies of the induced flow phenomena, we figured out that initially concentrated target molecules under the shrinking circular light pattern were washed out as the light pattern shrank because the concentrated region became smaller, resulting in a negative effect on the surface immunoreaction due to the decrease of local concentration of target molecules. On the other hand, a growing circular light pattern could dynamically transport target molecules to the temporally changed irradiated region without any loss of concentrated molecules at the reaction region under the dynamic optoelectrofluidic environment. As a result, the growing circular light pattern provided a binding efficiency of experimental results with a 2.18-fold enhancement compared to the passive mode, which exceeded the results of the static circular light pattern, having a 2.06-fold enhancement.

Conclusions

In this paper, a novel optoelectrofluidic enhanced immunoreaction system based on AC electroosmotic flow has been proposed and investigated with mathematical simulation studies and real experiments to solve the slow immunoreaction problem which is the most significant drawback faced in conventional surface-based assay platforms. When a light pattern was irradiated on the assay spot with an application of AC voltage, the optically-induced AC electroosmotic vortex flow continuously transported molecules into the assay spot from its surrounding regions. Consequently, the analyte depletion caused by diffusion limitations could be effectively overcome, resulting in more than two-fold enhancement of immunoreaction compared to the passive mode. We also investigated the effect of dynamic light patterns on optoelectrofluidic enhancement. As a result, the growing circular light pattern provided better binding efficiency than static light patterns due to the improved mass transport of target molecules, resulting in an achievement of a 2.18-fold enhancement for immunoreaction performance compared to the passive mode. In conclusion, our proposed system provides several advantages over previously reported studies of electrokinetic approaches for enhancing surface-based immunoassays with respect to the unnecessary need for complicated electrode fabrication which could not be adjustable to different dimensions of the reaction surface and

dynamically changed and the small volume of sample consumption. Furthermore, thanks to the simple optical control method for mass transport, this optoelectrofluidic system provides promising potential to be integrated with various types of microfluidic devices, including microarray formats for faster detection of small amounts of target molecules in biological fields such as disease diagnostics and biomarker discovery.

Acknowledgements

Notes and references

1 D. T. Okou, K. M. Steinberg, C. Middle, D. J. Cutler, T. J. Albert and M. E. Zwick, *Nat. Methods*, 2007, **4**, 907–909.

2 M. F. Templin, D. Stoll, J. M. Schwenk, O. Pötz, S. Kramer and T. O. Joos, *Proteomics*, 2003, **3**, 2155–2166.

3 J. Burke, E. B. Butler, B. S. Teh and B. B. Haab, *Proteomics*, 2003, **3**, 56–63.

4 B. I. Fall, B. Eberlein-König, H. Behrendt, R. Niessner, J. Ring and M. G. Weller, *Anal. Chem.*, 2003, **75**, 556–562.

5 T. M. Squires, R. J. Messinger and S. R. Manalis, *Nat. Biotechnol.*, 2008, **26**, 417–426.

6 M. Selmi, F. Echouchene, M. Gazzah and H. Belmabrouk, *IEEE Sens. J.*, 2015, **15**, 7321–7328.

7 K.-R. Huang, J.-S. Chang, S. D. Chao, K.-C. Wu, C.-K. Yang, C.-Y. Lai and S.-H. Chen, *J. Appl. Phys.*, 2008, **104**, 064702.

8 F. Kardous, A. Rouleau, B. Simon, R. Yahiaoui, J.-F. Manceau and W. Boireau, *Biosens. Bioelectron.*, 2010, **26**, 1666–1671.

9 N. S. Lynn Jr, M. Bocková, P. Adam and J. Homola, *Anal. Chem.*, 2015, **87**, 5524–5530.

10 I. F. Cheng, H. L. Yang, C. C. Chung and H. C. Chang, *Analyst*, 2013, **138**, 4656–4662.

11 C.-C. Wu and D.-J. Yang, *Biosens. Bioelectron.*, 2013, **43**, 348–354.

12 P. Y. Chiou, A. T. Ohta and M. C. Wu, *Nature*, 2005, **436**, 370–372.

13 D. Han, H. Hwang and J.-K. Park, *Appl. Phys. Lett.*, 2013, **102**, 054105.

14 H. Hwang and J. K. Park, *Lab Chip*, 2009, **9**, 199–206.

15 W. Choi, S.-W. Nam, H. Hwang, S. Park and J.-K. Park, *Appl. Phys. Lett.*, 2008, **93**, 143901.

16 H. Hwang, D.-H. Lee, W. Choi and J.-K. Park, *Biomicrofluidics*, 2009, **3**, 014103.

17 H. Hwang, Y. J. Choi, W. Choi, S. H. Kim, J. Jang and J. K. Park, *Electrophoresis*, 2008, **29**, 1203–1212.

18 H. Hwang and J. K. Park, *Anal. Chem.*, 2009, **81**, 5865–5870.

19 D.-H. Lee, H. Hwang and J.-K. Park, *Appl. Phys. Lett.*, 2009, **95**, 164102.

20 H. Hwang, D. Han, Y.-J. Oh, Y.-K. Cho, K.-H. Jeong and J.-K. Park, *Lab Chip*, 2011, **11**, 2518–2525.

21 H. Hwang, H. Chon, J. Choo and J.-K. Park, *Anal. Chem.*, 2010, **82**, 7603–7610.

22 A. Ramos, H. Morgan, N. G. Green and A. Castellanos, *J. Colloid Interface Sci.*, 1999, **217**, 420–422.

23 O. Hofmann, G. Voirin, P. Niedermann and A. Manz, *Anal. Chem.*, 2002, **74**, 5243–5250.

24 A. Sadana and D. Sii, *J. Colloid Interface Sci.*, 1992, **151**, 166–177.

25 W. M. Deen, *Analysis of Transport Phenomena, Topics in Chemical Engineering*, Oxford University Press, New York, 1998.